Improving Mode-Change and Fault Isolation of Hybrid System Using Instantaneous Sensitivity Matrices

Rami Levy and Shai Arogeti
Department of Mechanical Engineering
Ben-Gurion University of the Negev
Beer-Sheva, Israel
e-mails: arogeti@bgu.ac.il, levyram@post.bgu.ac.il

Danwei Wang
School of Electrical and Electronic Engineering
Nanyang Technological University
Singapore
e-mail: edwwang@ntu.edu.sg

***Abstract*—One approach to quantitative model-based fault detection and isolation (FDI) is based on analytical redundancy relations (ARRs) and fault signatures. Numerical evaluation of an ARR creates a residual, which then, provides online information on the consistency of the system and its nominal model. An inconsistency is represented by a signature. Traditionally in the quantitative approach, these signatures are binary vectors, where the term 0 means a residual is consistent and 1 means inconsistent. In this paper, the measured trend of residuals is utilized for FDI by a different type of signature, called sensitivity signature. In a sensitivity signature, the consistency of ARRs is represented by three terms; the term +1 indicates a residual is crossing an upper threshold, the term -1 indicates a residual is crossing a lower threshold and the term 0 means otherwise. The expected sensitivity signature related to a certain fault or to a mode change is taken from partial derivative of residuals. Fault isolation is a process where the measured signature is compared to signatures from the set of expected signatures. Since consistency, in the sensitivity approach, is represented by three terms (instead of two), more distinguished signatures are generated and improved fault and mode change isolation abilities are achieved.**

Keywords*—fault detection and isolation (FDI), mode-change isolation, sensitivity signature, sensitivity signature matrices, hybrid bond graph, hybrid systems.

I. INTRODUCTION

Among the many advantages of the bond graph (BG) model, many will consider its ability to represent causal relations between model variables in a clear and systematic way, as one of its major advantages. The ability to effectively analyze causal relations, makes the bond graph an excellent tool for FDI algorithms.

Complex physical systems may consist of different components with different dynamical nature (continuous and discrete). These systems are best modeled as hybrid systems. A hybrid system is represented by a set of modes. In each mode the system is represented by a continuous model and different modes correspond to different continuous models. In hybrid systems, two types of faults can be distinguished, these are, parametric faults and discrete faults. A parametric fault is related to a change of a physical parameter to an unknown abnormal value. On the other hand, discrete faults are due to inconsistency between the expected and the actual mode of the system. Bond graph theory was developed for modeling and analysis of continuous dynamical systems. An extension of this theory to hybrid systems was presented in [1], which has introduced the hybrid bond graphs (HBG). Fault diagnosis methods, based on the HBG modeling approach, can be found in [2, 3, 4, 5, 6, 7, 8, 9].

A fault diagnosis process is divided into three main stages: 1) detection of inconsistency between the behavior of the system and its nominal model, 2) isolation of a set of fault candidates and 3) identification of the true fault and its size. The search for an effective fault isolation method is very important in FDI framework. This effectiveness is measured by the complexity of the algorithm and its achieved isolation ability. Improved isolation ability demands, in general, a more complex method and a tradeoff between these two is unavoidable. In model-based process supervision, qualitative methods ([10]) are considered to be more computationally simple while quantitative methods are considered to be more reliable and provide better isolation ability ([11]). In model-based quantitative FDI methods, analytical redundancy relations (ARRs) are derived systematically from the systems model ([12, 13]). These model-based quantitative methods require online evaluation of ARRs, and the performance of the method depends on the quality model. Nevertheless, recent development of powerful micro-computers and the fact that an accurate model can be derived for many industrial applications make the model-based quantitative FDI methods attractive and feasible.

A numerical evaluation of an ARR generates a residual. In fault-free conditions, the residual value is theoretically zero. The residual value is nonzero in the presence of a fault, if the residual is sensitive to the occurred fault. An inconsistency is often detected by a threshold-based rule, such as $|residual| > threshold$, where the threshold can be a predetermined constant value ([4, 5, 14, 15, 16, 17]) or an adaptive threshold with a time varying value ([18, 19, 20]). A coherence vector is utilized to represent the fault signature; its standard form is $CV = [cv_1 cv_2 .. cv_r]^T$ where $cv_i \in \{0,1\}$ is a binary variable, representing the consistency of the redundancy relation with the index i (0 if it is consistent and 1 otherwise). The expected signature due to a certain fault is

Proceedings of the 1st International and 16th National Conference on Machines and Mechanisms (iNaCoMM2013), IIT Roorkee, India, Dec 18-20 2013

derived a priory (offline) and all possible signatures are presented in a matrix, known as the fault signature matrix (FSM) (or global FSM if the system is hybrid [4]). Fault diagnosis methods based on this strategy do not use important information hidden in residual trends (i.e., a rising residual or a falling residual). In this paper, residual trends are taken into account; a strategy which leads to a coherence vector of the form $CV = \left[cv_1 cv_2 ..cv_r\right]^T$, where $cv_i \in \{0,+1,-1\}$. The sign +1 indicates a residual is crossing an upper threshold while the sign -1 represents the opposite (i.e., crossing a lower threshold); the sign 0 represents consistency. This coherence vector is richer in information and therefore improves fault and mode-change isolation. It is clear that more unique signatures can be generated from a set of r redundancy relations; the maximum number of unique signatures is now 3^r (compared to 2^r, achieved from the standard binary representation). In a hybrid system diagnosis framework, the coherence vector expresses consistency (or inconsistency) of both, parametric faults and modes. An inconsistency may indicate an unexpected mode change, for instance, due to a discrete fault. Mode tracking and discrete fault isolation is based on the mode change signature and all possible mode change signatures are represented in a matrix, named, mode change signature matrix (MCSM) ([4]). This matrix, and the global FSM (GFSM) are derived offline from the HBG and represent cause-effect relations between parametric faults, mode changes and residuals. In this paper, due the new signature definition, these two matrices will be redefined in order to include the expected signatures of the new form.

In [21, 22], a qualitative fault isolation scheme, named TRANSEND, is presented. The isolation scheme is based on analyzing the transients in the measurements due to faults. The expected deviation is compared with the actual observed deviation. Fault signatures and the corresponding fault signature matrix are presented for a non-hybrid system, based on a qualitative model, named TCG.

In this paper, the expected residual trend due to a fault or due to a mode change is generated by explicit partial derivative of residuals. This information is presented in two signature matrices, which in general are time varying and replace the GFSM and the MCSM in their standard form.

Instead of explicit partial derivatives, sensitivity information of residuals can be derived by utilizing unique BG based numerical approaches, such as the sensitivity BG (SBG) ([23, 24]) or the incremental BG ([25, 26, 27]). These numerical approaches are more important in applications where the derivation of analytical residuals is not possible (e.g., due to algebraic loops). If an explicit representation of ARRs is not achievable, the diagnostic BG approach of [17] can be used, which has been shown to be extendable to the concept of SBG in [28] and to diagnosis of hybrid systems in [2]. From the practical aspect, explicit partial derivative of residuals can provide unreliable information due to model uncertainties, process disturbances and sensors noise. To overcome this difficulty, the choice of residual threshold is crucial. In most cases, constant thresholds can be applied with minimum false alarms and misdetections. However, if the uncertainties and disturbances obligate large threshold values, it would be preferred to apply adaptive threshold algorithms such as [18, 19, 20]. In order to minimize the effects of sensor noise on the partial derivatives, low-pass filters are suggested in this paper. Further investigation and validation is required in order to optimize practical use.

This paper is organized as follows. Section II reviews the diagnostic HBG modeling approach. Section III presents the concept of sensitivity signatures and sensitivity signature matrices. Section IV presents an example, where sensitivity signature matrices are derived. Section V shows simulation results and Section VI concludes the paper.

II. HYBRID MODELING FOR FAULT DIAGNOSIS

Analytical redundancy relations represent constraints between known process variables. The real time evaluation of ARRs generates residuals, which indicate on consistency between the system and its nominal model. ARRs can be derived systematically from a BG model and thus, many diagnosis methods are based on BG modeling theory ([13, 29, 17, 30]). The sensitivity of residuals to a change of a system parameter is represented by the fault signature matrix. An extension of this concept to hybrid systems is possible via the hybrid bond graph ([31, 1]). Since a HBG model tends to change its causal structure due to mode changes, the derivation of ARRs and FSMs was performed for each system mode independently. In order to handle this difficulty a diagnostic HBG with a consistent causality was introduced in [32, 33]. Such HBG allows global representation of constraint relations, and hence, global analytical redundancy relations (GARR) are derived and signatures can be represented in a global sense by the global fault signature matrix (GFSM). The GARR concept has paved the way for a systematic analysis and representation of mode change signatures, which are represented in the mode change signature matrix (MCSM).

In a diagnostic HBG, controlled junctions are represented by a unified description as described in Fig. 1. In this unified description, each controlled junction is associated with a binary state variable $a_i \in \{0,1\}$ that represents the junction state; 0 for an off junction (i.e., the junction is inactive) and 1 for an on junction (i.e., the junction is active). In a diagnostic HBG, the input variable of a controlled junction is defined as the product of the junction state variable (a_i) and the output variable of the neighbor X component (i.e., the component that is marked as X in Fig. 1. This representation restricts the X component to be an inactive component when the junction is off ([33]). An inactive bond-graph component is defined to be one of the following: an inactive controlled-junction, a null source (i.e. a source of zero effort or zero flow), or any other bond graph component such that any input variable of the component is an output variable of an off state controlled-junction. Any component that is not inactive is considered active. This method has been shown to be effective in several applications [2, 3, 34, 35].

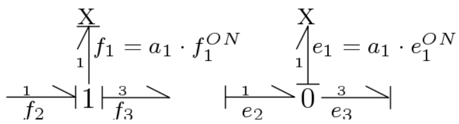

Fig. 1. Unified description of controlled junctions

A. Global Analytic Redundancy Relations

In a diagnostic HBG, all controlled junctions are assigned preferred causality for FDI. This preferred causality eliminates causality conflicts at the time of mode change. Due to the persistent causality structure, global ARRs, which represent constraint relations in a global sense (i.e., these relations are relevant to all modes) are derived. Controlled junction state variables take part in these global relations and their general form is $GARR = GARR(JV, CP, SO)$, where *JV* refers to controlled junction state variables (i.e., a_i values), *CP* includes component parameters and *SO* represents sensor output variables. An online evaluation of a GARR is a residual. If the absolute value of all residuals is below a threshold, the system is considered normal. If residuals show inconsistency, a fault is detected. A coherence vector $CV = [cv_1 cv_2 ...]^T$ is generated to show residuals inconsistency and the signature of the fault ($cv_i = 1$ if $GARR_i$ is inconsistent and zero otherwise). An evaluation of a GARR requires knowledge of the system's current mode. Therefore, as opposed to standard ARRs for FDI, the GARR has the ability to indicate inconsistency between the actual and expected mode of the system. This inconsistency causes a mode change signature, and if the new mode is not known, the mode change signature is utilized for a process of mode change isolation and identification. All cause-effect relations between residuals and mode changes are presented in the mode change signature matrix and all cause-effect relations between residuals and parametric faults are given in the global fault signature matrix.

B. Global Fault Signature matrix

The GFSM represents the relations between a predetermined set of parametric faults and their expected signatures. A typical structure of a GFSM is presented in Table. I. In a GFSM, each row represents a component parameters (i.e., p_i) and each column represents a GARR (i.e., $GARR_j$). In a standard FSM, each element $FSM_{ij} \in \{0,1\}$ is a binary value representing the sensitivity of the corresponding residual to a change in p_i. If FSMs are used for hybrid system diagnosis, these matrices are mode dependent and they are derived separately for each system's mode. The global FSM is different; since a single matrix is derived for all modes and the elements of this matrix are mode-dependent and presented as logical expressions of junction state variable. For example, if $GARR_1 = p_1 + a_1 p_2$ then the relevant values of the GFSM will be as follows:

$GFSM_{1,1} = 1$ meaning that $GARR_1$ is sensitive to a change in p_1 at all modes

$GFSM_{2,1} = a_1$ meaning that $GARR_1$ is sensitive to a change in p_2 only when $a_1 = 1$

We thus define the elements of the GFSM as follows: For any $i \in \{1..r\}$, $j \in \{1..n\}$, $i_1, i_2, ... i_k \in \{1..m\}$ where *r* is the number of GARRs in the system, *n* is the number of component parameters and *m* is the number of controlled junctions, we define:

$$GFSM_{ij} = \begin{cases} f(a_{i1}..a_{ik}), & \text{if the sensitivity of } GARR_j \text{ to a change in } p_i \text{ depends on the values of } a_{i1}...a_{ik} \\ 1, & \text{if } GARR_j \text{ is sensitive to a change in } p_i \text{ at all modes} \\ 0, & \text{otherwise} \end{cases} \quad (1)$$

where f is a logical function of controlled junction state variables. Two other columns, which represent fault detection and isolation abilities, can be added, and these abilities are, in general, mode dependent (These columns are not presented in Table I).

TABLE I. GLOBAL FAULT SIGNATURE MATRIX (GFSM)

	$GARR_1$	$GARR_2$	$\dots$	$GARR_r$
p_1	$GFSM_{1,1}$	$GFSM_{1,2}$	$\dots$	$GFSM_{1,r}$
p_2	$GFSM_{2,1}$	$GFSM_{2,2}$	$\dots$	$GFSM_{2,r}$
$\vdots$	$\vdots$	$\vdots$		$\vdots$
p_m	$GFSM_{m,1}$	$GFSM_{m,2}$	$\dots$	$GFSM_{m,r}$

C. Mode Change Signature Matrix

As mentioned, the GARRs are functions of controlled junction state variables, which represent the mode of the system. Thus, any inconsistency between the actual mode of the system and the values of controlled junction state variables (i.e., a_i) used in GARRs is indicated by residuals crossing thresholds. This indication is observed only in those GARR that have the inconsistent junction variables in the GARR expression, and hence, mode change signatures can be utilized for mode tracking and FDI of hybrid systems. All cause-effect relations between mode changes and GARRs are represented in the mode change signature matrix ([36]). A typical structure of the MCSM is presented in Table II. In the MCSM, each row represents a single junction state variable a_i, and each column represents a GARR (i.e., $GARR_i$). Every term $MCSM_{ij} \in \{0,1\}$ of the matrix has a binary value that indicates the sensitivity of $GARR_j$ to a mode change due to a change of the variable a_i. For every $i \in \{1..n\}$ and $j \in \{1..r\}$, where *n* is the number of controlled junctions and *r* is the number of GARRs, $MCSM_{ij}$ is defined as follows:

$$MCSM_{ij} = \begin{cases} 1, & \text{if } GARR_j \text{is a function of } a_i \\ 0, & \text{otherwise} \end{cases} \quad (2)$$

In this work, it is assumed that any change of mode is detectable by at least one GARR. This assumption means that no row of the MSCM is completely zero.

TABLE II. MODE CHANGE SIGNATURE MATRIX (MCSM)

	$GARR_1$	$GARR_2$	$\ldots$	$GARR_r$
a_1	$MCSM_{1,1}$	$MCSM_{1,2}$	$\ldots$	$MCSM_{1,r}$
a_2	$MCSM_{2,1}$	$MCSM_{2,2}$	$\ldots$	$MCSM_{2,r}$
$\vdots$	$\vdots$	$\vdots$		$\vdots$
a_n	$MCSM_{n,1}$	$MCSM_{n,2}$	$\ldots$	$MCSM_{n,r}$

III. INSTANTANEOUS SENSITIVITY SIGNATURE MATRICES

The instantaneous sensitivity signature matrices, presented in this paper, show the expected residual trends due to a parametric fault or due to a mode change. This concept extends the standard binary representation of signatures, such that the new associated coherence vector is defined as $CV = [cv_1 cv_2 .. cv_r]$ where $cv_i \in \{0, +1, -1\}$. Here, the sign +1 indicates on a residual that is crossing an upper (positive) threshold, while the sign -1 indicates on the crossing of a lower (negative) threshold. This new type of signature is named here sensitivity signature since it can be analyzed by sensitivity theory as in [23, 28, 37, 38]. In this paper, expected sensitivity signatures are taken from the instantaneous sign of residuals partial derivative, with respect to the inconsistent parameter. Thus, the elements of the sensitivity signature matrices are time varying and are calculated online. The set of all possible values in a sensitivity signature matrix is $\{0, +1, -1\}$. These values are the expected residual trend due to a parametric fault or due to a mode change. Two sensitivity signature matrices are defined, the first one is the global fault sensitivity signature matrix (GFSSM) and the second is the mode change sensitivity signature matrix (MCSSM). These matrices extend the GFSM and the MCSM as described in earlier section. The elements of the GFSSM are defined as follows:

$$GFSSM_{ij} = \begin{cases} -\text{sign}\left(\dfrac{\partial r_j}{\partial p_i}\right), & \text{if } r_j \text{ is a function of } p_i \text{ and } p_i \text{ is expected to increase due to a fault} \\ \text{sign}\left(\dfrac{\partial r_j}{\partial p_i}\right), & \text{if } r_j \text{ is a function of } p_i \text{ and } p_i \text{ is expected to decrease due to a fault} \\ 0, & \text{if } r_j \text{ is not a function of } p_i \end{cases} \quad (3)$$

where r_j is the residual of the j^{th} column and p_i is the parameter of the i^{th} row. The minus sign is explained as follows. When one of the parameters in the real system changes, the residual feels the opposite of this change. For example, if due to a fault, p_i has increased compared to its nominal value, the nominal value of p_i that is still used in the residual is lower than the real (faulty) value. It is then concluded that if the instantaneous partial derivative is positive and a real parameter is increasing, this will be observed as a decrease in the residual value, and vice versa. A parameter of a system component may increase or decrease due to a fault. For some parameters, e.g., due to some physical constraints, only one direction would be feasible. Consider for example a tank filled with liquid, and the only possible fault related to this tank is a leakage (assuming that the tank is covered and contains liquids only). If this tank is modeled as a capacitive element (i.e., C) in a BG model with the parameter *C* (representing the tank capacitance), then the leakage fault is represented as an increase of *C*. In this case, a fault that is represented as a decrease of *C* is not feasible and this information should be used in the fault isolation process. Hence, the GFSSM uses a new notation, which distinguishes between a fault of an increasing parameter, represented as $p_i \uparrow$, and a fault of a decreasing parameter that is represented by $p_i \downarrow$. For mode-change isolation, this kind of distinction is also very important and may improve mode-change isolation ability. If the state of a junction is (for example) $a_i = 0$, the value of a_i may increase (to $a_i = 1$), but it definitely would not decrease. This information is useful for mode change isolation, and hence, the elements of the MCSSM are defined in the following way:

$$MCSSM_{ij} = \begin{cases} -\text{sign}\left(\dfrac{\partial r_j}{\partial a_i}\right), & \text{if } r_j \text{ is a function of } a_i \text{ and } a_i = 0 \\ \text{sign}\left(\dfrac{\partial r_j}{\partial a_i}\right), & \text{if } r_j \text{ is a function of } a_i \text{ and } a_i = 1 \\ 0, & \text{if } r_j \text{ is not a function of } a_i \end{cases} \quad (4)$$

where r_j is the residual of the j^{th} column and a_i is the junction state variable of the i^{th} row.

IV. EXAMPLE

The two-tank system presented in Fig. 2 is now considered as an example. The system consists of two sensors (a pressure-sensor p_1 and a flow-sensor f), an ON/OFF controller (which regulates the level in tank C_1 between two levels h_{min} and h_{max} as illustrated in Fig. 3, a pump (that is a source of flow), a drainage and two consumer valves A and B. Each valve could be in one of two discrete states, open or closed. This system (Fig. 2) is also presented in [6], as a case study, where the causality assignment procedure of a diagnostic hybrid bond graph is demonstrated. The diagnostic HBG of the system in Fig. 2 is presented in Fig. 4 (for more details the reader may refer to [6]). In this model, a_1 represents the discrete state of the pump, a_2 represents the discrete state of the drainage and the two variables a_3, a_4 represent the discrete state of the valves A and B, respectively. The two tanks are modeled as linear capacitive C elements with the parameters C_1 and C_2. The valves, drainage and pipe (between the two tanks) are modeled as resistive R elements with the coefficients R_1 for the drainage, R_2 for the pipe and R_3, R_4 for the consumer valves A and B, respectively.

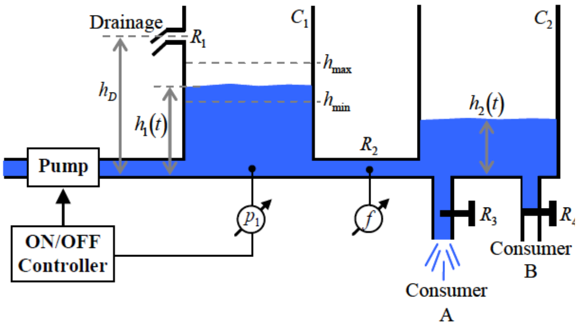

Fig. 2. The two-tank plant

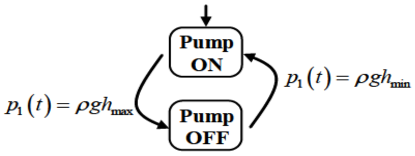

Fig. 3. The ON/OFF controller

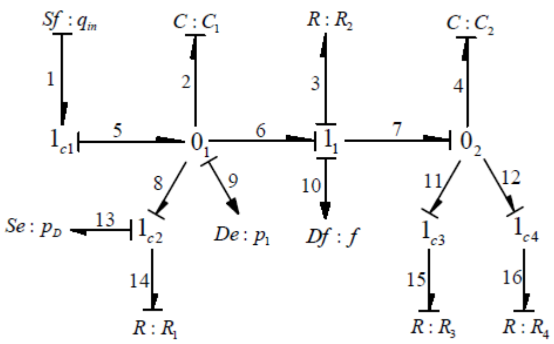

Fig. 4. A diagnostic HBG of the two-tank system

In order to simplify the description of the method, a linear relation between effort (pressure) and flow is assumed here for all resistive elements (i.e., valves, drainage and pump). With this assumption, the two GARRs are derived from the constitutive equations of the two junctions 0_1 and 0_2, as follows:

$$GARR_1 \Rightarrow$$
$$r_1 = a_1 q_{in} - C_1 \dot{p}_1 - f - a_2 (p_1 - p_D) / R_1 \tag{5}$$

$$GARR_2 \Rightarrow$$
$$r_2 = f - C_2 (\dot{p}_1 - R_2 \dot{f}) - \left(\frac{a_3}{R_3} + \frac{a_4}{R_4} \right) (p_1 - R_2 f) \tag{6}$$

According to (3) and (4), the corresponding sensitivity matrices are presented in Table III and in Table IV. As mentioned above, the rows of the GFSSM represent faults with a specified tendency. With respect to the two tanks, the only feasible faults related to C_1 and C_2 are assumed to be $C_1 \uparrow$ and $C_2 \uparrow$ (i.e., only leakage faults). For all other parameters (i.e., $R_1, R_2, R_3, R_4, q_{in}$), both increasing and decreasing faults are possible.

TABLE III. GLOBAL FAULT SENSITIVITY SIGNATURE MATRIX

	$GARR_1$	$GARR_2$
$R_1 \uparrow$	$-a_2 \mathrm{sign}(p_1 - p_D) / R_1^2$	0
$R_1 \downarrow$	$a_2 \mathrm{sign}(p_1 - p_D) / R_1^2$	0
$R_2 \uparrow$	0	$\mathrm{sign}(C_2 \dot{f} + (a_3 / R_3 + a_4 / R_4) f)$
$R_2 \downarrow$	0	$\mathrm{sign}(C_2 \dot{f} + (a_3 / R_3 + a_4 / R_4) f)$
$R_3 \uparrow$	0	$-a_3 \mathrm{sign}(a_3 (p_1 - R_2 f) / R_3^2)$
$R_3 \downarrow$	0	$a_3 \mathrm{sign}(a_3 (p_1 - R_2 f) / R_3^2)$
$R_4 \uparrow$	0	$-a_4 \mathrm{sign}(a_4 (p_1 - R_2 f) / R_4^2)$
$R_4 \downarrow$	0	$a_4 \mathrm{sign}(a_4 (p_1 - R_2 f) / R_4^2)$
$C_1 \uparrow$	$\mathrm{sign}(\dot{p}_1)$	0
$C_2 \uparrow$	0	$\mathrm{sign}(\dot{p}_1 - R_2 \dot{f})$
$q_{in} \uparrow$	$-a_1$	0
$q_{in} \downarrow$	a_1	0

TABLE IV. MODE CHANGE SENSITIVITY SIGNATURE MATRIX

	$GARR_1$	$GARR_2$
a_1	$\begin{cases} -\mathrm{sign}(q_{in}), & \text{if } a_1 = 0 \\ \mathrm{sign}(q_{in}), & \text{if } a_1 = 1 \end{cases}$	0
a_2	$\begin{cases} \mathrm{sign}\left(\frac{(p_1 - p_D)}{R_1}\right), & \text{if } a_2 = 0 \\ -\mathrm{sign}\left(\frac{(p_1 - p_D)}{R_1}\right), & \text{if } a_2 = 1 \end{cases}$	0
a_3	0	$\begin{cases} \mathrm{sign}\left(\frac{(p_1 - R_2 f)}{R_3}\right), & \text{if } a_3 = 0 \\ \text{-sign}\left(\frac{(p_1 - R_2 f)}{R_3}\right), & \text{if } a_3 = 1 \end{cases}$
a_4	0	$\begin{cases} \mathrm{sign}\left(\frac{(p_1 - R_2 f)}{R_4}\right), & \text{if } a_4 = 0 \\ \text{-sign}\left(\frac{(p_1 - R_2 f)}{R_4}\right), & \text{if } a_4 = 1 \end{cases}$

V. SIMULATION RESULTS

The two-tank system of the example was simulated using the MATLAB Simulink software. The nominal parameters of this system are presented in the appendix. The simulation stop-time is 300[sec], and during this time interval a few faults (parametric and discrete) were injected into the system. The simulated behavior of the variable a_1 is due to the ON/OFF control law, the state of the variable a_2 (which represents the state of the drainage) was changed when the fluid level has crossed h_D, and the variables a_3, a_4 were changed randomly in all 4 possible combinations. The simulated measurements p_1 and f are presented in Fig. 5 and the online values of the residuals are presented in Fig. 6. The time history of all four controlled junction state variables a_1, a_2, a_3 and a_4 are presented in Fig. 7, together with the time history of the measured signatures, represented by the coherence vector (CV). These values were filtered in order to remove unwanted spikes that appear in the residuals due to numerical approximations. Four fault scenarios are presented: 1) A single parametric fault of a decreasing R_3 parameter (e.g., due to a valve leakage). 2) A single discrete fault of $a_1 = 1$ (at a time where $a_1 = 0$ is expected), this fault is due to a stuck ON pump (which consequently causes liquid flow through the drainage outlet). 3) A simultaneous discrete and parametric fault, as a decreasing R_3 fault (due to a pipe leakage) is injected while the pump is stuck ON. And lastly, 4) a single parametric fault of an increasing R_2 parameter (i.e., a pipe blockage). The size and timing of all faults are presented in Table. V.

The fault isolation process is carried out by comparing the measured signature (in the vector CV) with the instantaneous rows of the GFSSM and the MCSSM. All matching results are collected to a set of fault and mode-change candidates. If the set of fault candidates includes a single candidate, then this fault is a certain fault; otherwise, the faults in the set are uncertain faults. In general, this work assumes only a single fault in the system at any point of time (i.e., this is the single fault assumption). However, it is clear that also multiple fault isolation may benefit from the new approach and this argument is supported by the results of the third fault scenario.

The simulated sensitivity signatures and the instantaneous sensitivity signature matrices were sampled at relevant points in time and the results are presented in Table. VI (GFSSM is presented above the dashed line and MCSSM is below). Note that the standard binary signatures that would have achieved if only GFSM and MCSM were considered, are equal to the absolute value of the presented sensitivity signatures. A discussion about these results and the improved isolation ability achieved for each fault scenario is presented as follows.

- According to the simulated signature (i.e., the vector CV) due to the fault $R_3\downarrow$, the isolated fault candidates (based on the instantaneous information of the GFSSM) are: $R_2\uparrow$, $R_3\downarrow$, $R_4\downarrow$. If the residual trends were not considered in the isolation process, the isolated fault and mode-change candidates were: R_2, R_3, R_4, a_3, a_4.

- According to the simulated signature due to the fault related to a_1, the isolated certain fault is a_1 (this result is based on the instantaneous information of the MCSSM). If the residual trends were not considered in the isolation process, the isolated fault and mode-change candidates were: C_1, a_1, a_2.

- According to the simulated signature due to the fault $R_2\downarrow$, while a discrete fault a_1 is also present, the isolated certain fault is $R_2\downarrow$ (since $cv_2 = -1$ is possible only for $R_2\downarrow$) and the uncertain fault and mode-change candidates are: $R_1\uparrow$ (based on the GFSSM), a_1, a_2 (from the MCSSM). If the residual trends were not considered in the isolation process, the isolated fault and mode-change candidates were: $R_1, R_2, C_1, C_2, a_1, a_2$.

- According to the simulated signature due to the fault $R_2\uparrow$, the isolated certain fault is $R_2\uparrow$ (using the GFSSM information). If the residual trends were not considered in this process, the isolated fault and mode-change candidates were: R_2, C_2, a_3, a_4.

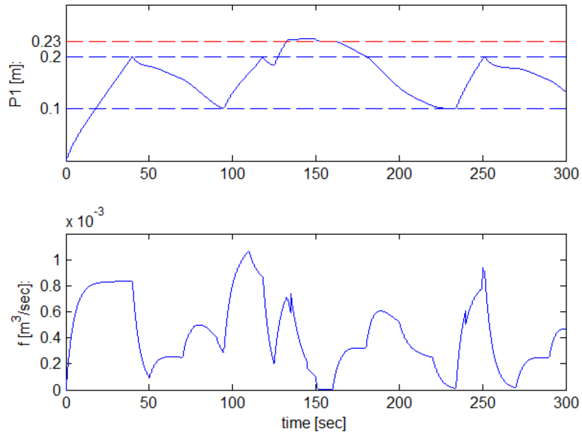

Fig. 5. Simulated measurements

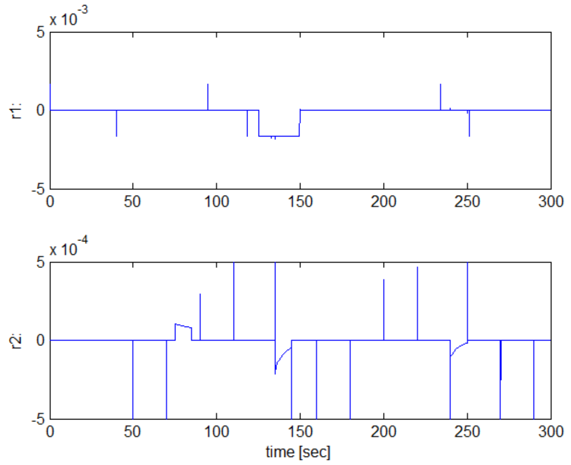

Fig. 6. Simulated residuals

TABLE V. SIMULATED FAULTS

	Description	Injected value	Start time	End time
$R_3\downarrow$	valve leakage	$0.8R_3$	75	85
a_1	stuck ON pump	$\overline{a_1}$	120	150
$R_2\downarrow$	pipe leakage	$0.8R_2$	135	145
$R_2\uparrow$	pipe blockage	$1.2R_2$	240	250

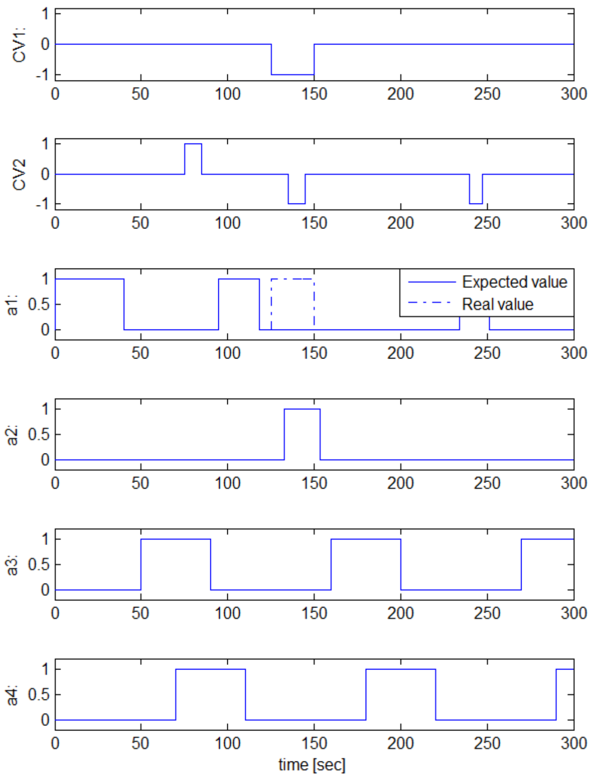

Fig. 7. Junction switch state variables and coherence vectors

VI. Conclusions

In this paper, a fault and mode-change isolation method, based on fault sensitivity signatures, is presented for hybrid system diagnosis. The new method uses information of residual trends, and the considered signatures are defined with three signs (+1,-1,0). In this method a rising residual is distinguished from a falling residual and this extra information is utilized for improved isolation abilities. The implementation of the method requires two time varying matrices, the global fault sensitivity signature matrix (GFSSM) and the mode change sensitivity signature matrix (MCSSM). The first matrix represents instantaneous cause-effect relations between parametric faults and residuals while the second matrix represents instantaneous relations between mode-changes and residuals. These matrices show expected signatures which are defined by three signs (+1,-1,0). An example of a two-tank system is presented, and the simulation results demonstrate the advantages of the new method. From the practical aspect, the suggested method can be implemented by other unique BG based numerical approaches, rather than explicit partial derivatives of the residuals. Furthermore, an industrial implementation should consider model uncertainties, process disturbances and sensor noise, e.g., by utilizing adaptive threshold and filtering algorithms. These elements will investigated in future work.

TABLE VI. Instantaneous Sensitivity Signature Matrices and Simulated Signatures Achived in CV

	t=75.1[sec]		t=125.1[sec]		t=135.1[sec]		t=240.1[sec]	
	$GARR_1$	$GARR_2$	$GARR_1$	$GARR_2$	$GARR_1$	$GARR_2$	$GARR_1$	$GARR_2$
$R_1\uparrow$	0	0	0	0	-1	0	0	0
$R_1\downarrow$	0	0	0	0	1	0	0	0
$R_2\uparrow$	0	1	0	1	0	1	0	-1
$R_2\downarrow$	0	-1	0	-1	0	-1	0	1
$R_3\uparrow$	0	-1	0	0	0	0	0	0
$R_3\downarrow$	0	1	0	0	0	0	0	0
$R_4\uparrow$	0	-1	0	0	0	0	0	0
$R_4\downarrow$	0	1	0	0	0	0	0	0
$C_1\uparrow$	-1	0	1	0	1	0	1	0
$C_2\uparrow$	0	-1	0	1	0	1	0	1
$q_{in}\uparrow$	0	0	0	0	0	0	-1	0
$q_{in}\downarrow$	0	0	0	0	0	0	1	0
a_1	-1	0	-1	0	-1	0	1	0
a_2	1	0	1	0	-1	0	1	0
a_3	0	-1	0	1	0	1	0	1
a_4	0	-1	0	1	0	1	0	1
CV	0	1	-1	0	-1	-1	0	-1

Acknowledgment

This work was supported by the Israel Science Foundation under Grant 1278/10.

References

[1] P.J. Mosterman and G. Biswas, "Behavior generation using model switching a hybrid bond graph modeling technique," SIMULATION SERIES, 27:177-177, 1994.

[2] R. Levy, S. Arogeti, and D. Wang, "An integrated approach to mode tracking and diagnosis of hybrid systems," IEEE Transactions on Industrial Electronics, in press.

[3] S.A. Arogeti, D. Wang, C.B. Low, and M. Yu, "Fault detection isolation and estimation in a vehicle steering system," IEEE Transactions on Industrial Electronics, 59(12):4810-4820, 2012.

[4] S.A. Arogeti, D. Wang, and C.B. Low, "Mode identification of hybrid systems in the presence of fault," IEEE Transactions on Industrial Electronics, 57(4):1452-1467, 2010.

[5] S.A. Arogeti, D. Wang, and C.B. Low, "Mode tracking and FDI of hybrid systems," in 10th International Conference on Control, Automation, Robotics and Vision, pp. 892-897. IEEE, 2008.

[6] C.B. Low, D. Wang, S. Arogeti, and J.B. Zhang, "Causality assignment and model approximation for hybrid bond graph: Fault diagnosis perspectives," IEEE Transactions on Automation Science and Engineering, 7(3):570-580, 2010.

[7] C.B. Low, D. Wang, S.A. Arogeti, and M. Luo, "Fault parameter estimation for hybrid systems using hybrid bond graph," in Control Applications, (CCA) Intelligent Control, (ISIC), 2009 IEEE, pp. 1338-1343, July 2009.

[8] M.J. Daigle, X.D. Koutsoukos, and G. Biswas, "An event-based approach to integrated parametric and discrete fault diagnosis in

hybrid systems," Transactions of the Institute of Measurement and Control, 32(5):487, 2010.

[9] S. Narasimhan and G. Biswas, "Model-based diagnosis of hybrid systems," IEEE Transactions on Systems, Man and Cybernetics, Part A: Systems and Humans, 37(3):348-361, 2007.

[10] V. Venkatasubramanian, R. Rengaswamy, and S.N. Kavuri, "A review of process fault detection and diagnosis: Part II: Qualitative models and search strategies," Computers & Chemical Engineering, 27(3):313-326, 2003.

[11] V. Venkatasubramanian, R. Rengaswamy, K. Yin, and S.N. Kavuri, "A review of process fault detection and diagnosis: Part I: Quantitative model-based methods," Computers & chemical engineering, 27(3):293-311, 2003.

[12] J. Gertler, "Analytical redundancy methods in fault detection and isolation," in proceedings of IFAC/IAMCS symposium on safe process, volume 1, pp. 9-21, 1991.

[13] B. Ould Bouamama, A.K. Samantaray, M. Staroswiecki, and G. Dauphin-Tanguy, "Derivation of constraint relations from bond graph models for fault detection and isolation," 2003. ICBGM'03, Jan 2003, Orlando, Simulation Series, Vol. 35, Number 2, SCS Publication, pp.104-109.

[14] K. Medjaher, A.K. Samantaray, B. Ould Bouamama, and M. Staroswiecki, "Supervision of an industrial steam generator. Part II: Online implementation," Control engineering practice, 14(1):85-96, 2006.

[15] B. Ould Bouamama, K. Medjaher, A.K. Samantaray, and M. Staroswiecki, "Supervision of an industrial steam generator. Part I: Bond graph modelling," Control engineering practice, 14(1):71-83, 2006.

[16] K. Medjaher, "A bond graph model-based fault detection and isolation," Maintenance Modelling and Applications, chapter 6: Fault Diagnostics, pp. 503-512, 2011.

[17] A.K. Samantaray, K. Medjaher, B. Ould Bouamama, M. Staroswiecki, and G. Dauphin-Tanguy, "Diagnostic bond graphs for online fault detection and isolation," Simulation Modelling Practice and Theory, 14(3):237-262, 2006.

[18] S.K. Ghoshal, S. Samanta, and A.K. Samantaray, "Robust fault detection and isolation of hybrid systems with uncertain parameters," Proceedings of the Institution of Mechanical Engineers, Part I: Journal of Systems and Control Engineering, 226(8):1013-1028, 2012.

[19] M.A. Djeziri, R. Merzouki, B. Ould Bouamama, and G. Dauphin-Tanguy, "Bond graph model based for robust fault diagnosis," in American Control Conference (ACC'07), pp. 3017-3022. IEEE, 2007.

[20] S.X. Ding, "Norm-based residual evaluation and threshold computation," in Model-Based Fault Diagnosis Techniques, pp. 285-313. Springer, 2013.

[21] A. Bregon, B. Pulido, and G. Biswas, "Efficient on-line fault isolation and identification in TRANSCEND for nonlinear systems," in proceedings of the 20th international workshop on principles of diagnosis, DX09, pp. 291-298, 2009.

[22] G. Biswas, X. Koutsoukos, A. Bregon, and B. Pulido, "Analytic redundancy, possible conflicts, and TCG-based fault signature diagnosis applied to nonlinear dynamic systems," in proceedings of the 7th IFAC symposium on fault detection, supervision, and safety of technical processes (SAFEPROCESS 2009), pp. 1486, 2009.

[23] P.J. Gawthrop, "Sensitivity bond graphs," Journal of the Franklin Institute, 337(7):907-922, 2000.

[24] P.J. Gawthrop and E. Ronco, "Estimation and control of mechatronic systems using sensitivity bond graphs," Control Engineering Practice, 8(11):1237-1248, 2000.

[25] W. Borutzky, "Incremental bond graphs," in Bond graph modelling of engineering systems, pp. 135-176. Springer, 2011.

[26] W. Borutzky, "Parameter sensitivities of transfer functions and of residuals," in proceedings of the 2010 Spring Simulation Multiconference, pp. 202. Society for Computer Simulation International, 2010.

[27] W. Borutzky and J Granda, "Bond graph based frequency domain sensitivity analysis of multidisciplinary systems," in proceedings of the Institution of Mechanical Engineers, Part I: Journal of Systems and Control Engineering, 216(1):85-99, 2002.

[28] A.K. Samantaray and S.K. Ghoshal, "Sensitivity bond graph approach to multiple fault isolation through parameter estimation," in proceedings of the Institution of Mechanical Engineers, Part I: Journal of Systems and Control Engineering, 221(4):577-587, 2007.

[29] M. Tagina, J.P. Cassar, G. Dauphin-Tanguy, and M. Staroswiecki, "Monitoring of systems modelled by bond graph," 1995. in: Proc. ICBGM'95, Simulation Series, vol. 27, no. 1, 1995, pp. 275-280, ISBN: 1-56555-037-4.

[30] A.K. Samantaray and B. Ould Bouamama. Model-based process supervision: a bond graph approach. Springer Verlag, 2008.

[31] P.J. Mosterman and G. Biswas, "A theory of discontinuities in physical system models," Journal of the Franklin Institute, 40(6):966-979, 1996.

[32] C.B. Low, D. Wang, S. Arogeti, and J.B. Zhang, "Monitoring ability analysis and qualitative fault diagnosis using hybrid bond graph," in proceedings of the 17th World Congress, pp. 10516-10521, 2008.

[33] S. Arogeti, D. Wang, C.B. Low, H.D. Zhang, and J. Zhou, "Mode tracking of hybrid systems in FDI framework," in IEEE Conference on Robotics, Automation and Mechatronics, pp. 841-846., 2008.

[34] S. Arogeti, D. Wang, C. B. Low, and M. Yu, "Fault detection and isolation in a mobile robot test-bed," in: Advanced Intelligent Mechatronics, 2009. AIM 2009. IEEE/ASME International Conference on, pp. 398-404. IEEE, 2009.

[35] C.B. Low, D. Wang, S. Arogeti, and M. Luo, "Quantitative hybrid bond graph-based fault detection and isolation," IEEE Transactions on Automation Science and Engineering, 7(3):558-569, 2010.

[36] S.A. Arogeti, D. Wang, and C.B. Low, "Mode tracking and FDI of hybrid systems," in: 10th International Conference on Control, Automation, Robotics and Vision (ICARCV'2008), pp. 892-897, 2008.

[37] R. Tomovic and M. Vukobratovic, General Sensitivity Theory, volume 35 of Modern analytic and computational methods in science and mathematics, New York, 1972.

[38] P.M. Frank, Introduction to System Sensitivity Theory, Academic Press, New York, 1978.

APPENDIX

TABLE VII. NOMINAL SYSTEM PARAMETERS

Variable	Description	Value	Start time
R_1	drainage flow coefficient	3	$\left[\frac{\mathrm{m}}{\mathrm{m}^3/\mathrm{sec}}\right]$
R_2	pipe flow coefficient	50	$\left[\frac{\mathrm{m}}{\mathrm{m}^3/\mathrm{sec}}\right]$
R_3	valve A flow coefficient	300	$\left[\frac{\mathrm{m}}{\mathrm{m}^3/\mathrm{sec}}\right]$
R_4	valve B flow coefficient	200	$\left[\frac{\mathrm{m}}{\mathrm{m}^3/\mathrm{sec}}\right]$
C_1	tank 1 cross-section	0.185	$\left[\mathrm{m}^2\right]$
C_2	tank 2 cross-section	0.185	$\left[\mathrm{m}^2\right]$
q_{in}	volumetric flow rate of pump	0.00166	$\left[\mathrm{m}^3/\mathrm{sec}\right]$
h_{min}	maximum fluid level	0.2	$[\mathrm{m}]$
h_{max}	minimum fluid level	0.1	$[\mathrm{m}]$
$h_d (= P_D)$	drainage level	0.23	$[\mathrm{m}]$